Journal of Applied Polymer Science

Polyvinylbutyral-assisted synthesis and characterization of SnS mesoporous fibers via electrospinning process

Kuo-Chin Hsu,[1] Dong-Yang Wu,[2] Pei-Ying Lin,[3] Yaw-Shyan Fu,[2] Jiuun-Der Liao[1]

[1]Department of Materials Science and Engineering, National Cheng Kung University, Tainan 701, Taiwan
[2]Department of Greenergy, National University of Tainan, Tainan 701, Taiwan
[3]Department of Photonics, National Cheng Kung University, Tainan 701, Taiwan
Correspondence to: Y.-S. Fu (E-mail: ysfu@mail.nutn.edu.tw) and J.-D. Liao (E-mail: jdliao@mail.ncku.edu.tw)

ABSTRACT: Tin sulfide (SnS) has the potential to be used as a low-cost absorber material for applications in thin film photovoltaic solar cells. In this study, polyvinylbutyral/SnS (PVB/SnS) composite fibers were synthesized through a relatively simple electrospinning process. SnS mesoporous fibers were obtained from PVB/SnS composite fibers after sintering treatment at 500°C for 1 h in N_2 atmosphere. The SnS mesoporous fibers were then characterized using X-ray powder diffraction, scanning electron microscopy, thermogravimetric analysis, and transmission electron microscopy. The optical properties of SnS mesoporous fibers were also recorded by UV–vis absorption spectroscopy. The results showed that the synthesized SnS mesoporous fibers exhibited a single phase, stoichiometric composition, with good crystallinity, a size ranging from 100 to 200 nm, and a band gap of 1.49 eV. The as-prepared SnS mesoporous fibers are thus a suitable material to achieve visible light absorption in a thin film solar cell. © 2015 Wiley Periodicals, Inc. J. Appl. Polym. Sci. **2015**, *132*, 42388.

KEYWORDS: electrospinning; fibers; properties and characterization

Received 27 October 2014; accepted 20 April 2015
DOI: 10.1002/app.42388

INTRODUCTION

Tin sulfide (SnS) has attracted much attention, as compared to other IV–VI groups with narrow band gap semiconductors such as PbS, PbTe, and SnTe, because its constituent elements are abundant in nature and do not pose any health or environmental hazards.[1] SnS can be used in the fabrication of highly efficient solar cells,[2,3] while its non-toxic characteristic is of great importance for the photovoltaic industry, as compared with currently available CdTe and $CuInSe_2$ materials. In the past few years, several techniques have been employed for the preparation of SnS materials, such as spray pyrolytic deposition,[4] two-stage process,[5] thermal evaporation method,[6] chemical vapor deposition method,[7] electro-deposition method,[8] and solvothermal method.[9] However, to the best of our knowledge, there have not been any reports on the synthesis SnS fibers. In addition, one-dimensional nanostructures, such as nanofibers, nanorods, and nanotubes, have been the focus of much research interest due to their relatively large length to diameter ratios, as seen in a number of natural organic/inorganic materials.[10] On the other hand, one-dimensional nanofibers prepared by the electrospinning process are able to form a number of different synthetic fibers that show good potential for practical applications.[11–13] For example, polyvinylbutyral (PVB) can be used as a mesopore template, with the advantages of being non-toxic, odorless, and environmentally benign.[14,15] This polymer is thus widely used as a functional material in various fields, and is an excellent organic component to be utilized in the synthesis of organic/inorganic hybrid composites.

SnS is one of the tin chalcogenide layered semiconductors in groups IV–VI. It has a direct energy bandgap of 1.3–1.5 eV, close to the optimum value required for efficient light absorption and it has a high optical absorption coefficient for photons with energies greater than 1.3 eV.[16] Increasing the energy gap of the absorber layer can reduce the dark current and increase the open current voltage. But the high energy gap will reduce the efficiency of light absorption and therefore the most appropriate value E_g =1.3–1.5 eV. In this study, PVB/SnS composite fibers are first synthesized through an electrospinning process. The structure of the resulting SnS mesoporous fibers is then optimized by a sintering treatment to obtain a band gap energy that is suitable for light absorption in a thin film solar cell.

EXPERIMENTAL

Materials

The stannous chloride ($SnCl_2{\cdot}2H_2O$) used in this work was obtained from Merck KGaA (Darmstadt, Germany). Thiourea

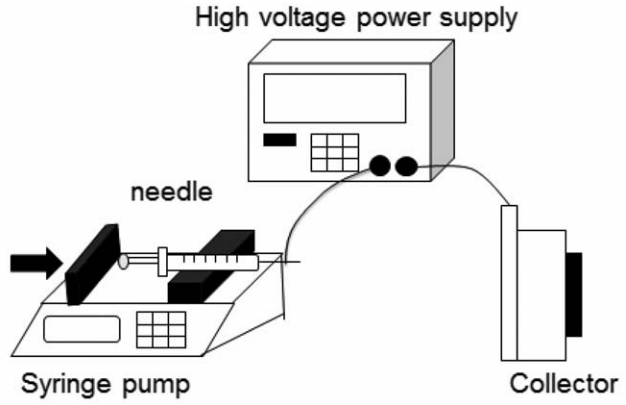

Figure 1. Schematic diagram of the applied electrospinning device.

(CH_4N_2S) was purchased from Alfa Aesar (Ward Hill, MA, USA), while PVB (average M_v ~40 kDa) was obtained from Chang Chun Group Company (Kaohsiung, Taiwan). Ethanol (99%) was purchased from PA Panreac (Barcelona, Spain), and the deionized water (DI water) used in this work was obtained from EMD Millipore Corporation, and produced using the Direct-Q 3 system (Billerica, MA).

Preparation of the Electrospinning Solution and SnS Fibers

In a typical synthesis, 1 mmol of $SnCl_2{\cdot}2H_2O$, 2 mmol of CH_4N_2S, and 6–10 wt % PVB were dissolved in 10 mL ethanol under magnetic stirring at room temperature for 2 h to obtain a homogenous precursor of PVB/SnS composites. A schematic setup of the electrospinning route used in this study is shown in Figure 1. The electrospinning setup consisted of a syringe and needle (with an internal diameter of 0.21 mm), a syringe pump (KD Scientific Inc., Model 200, Holliston, MA), a high positive voltage power supply (You-Shang Technical Corp., Kaohsiung, Taiwan), and a collection board. A stainless steel electrode was connected to a high voltage power supply, which could provide a DC voltage of up to 30 kV. Homogeneous PVB/SnS composite precursor solutions were prepared and immediately used for electrospinning. The as-prepared PVB/SnS composite fibers thus obtained were then transferred to a combustion boat, and calcined at 300–500°C for 1 h in N_2 atmosphere.

Characterization of PVB/SnS Composite Fibers

The X-ray powder diffraction (XRD, operating at 8 kV) patterns of the as-prepared samples were recorded on a Shimadzu XRD-6000 X-ray diffractmeter (Kyoto, Japan) with Cu Kα radiation ($\lambda = 0.15418$ nm). The morphologies and micro-/nanostructures were investigated with a HITACHI 4200A (Tokyo, Japan) scanning electron microscope (SEM, operating at 10 kV) and JEOL JEM-2000EX (Tokyo, Japan) transmission electron microscope (TEM, operating at 160 kV). The energy dispersive spectrometer (EDS) measurements were performed using a Horiba EX220 (Kyoto, Japan), which was attached to TEM for compositional analyses. Thermal analysis was carried out with a Perkin Elmer Pyris Diamond TG/DTA thermal analyzer (Boston, MA) in N_2 atmosphere at a heating rate of 20°C/min. UV–vis absorption spectra were recorded on a Hitachi U-3010 spectrophotometer (Tokyo, Japan).

RESULTS AND DISCUSSION

Morphologies of the Electrospun PVB/SnS Composite Fibers

Figure 2 shows SEM images of PVB/SnS composite fibers with different PVB concentrations of (a) 6, (b) 7, (c) 8, (d) 9, and (e) 10%. Figure 2(a) shows that a few beaded structures appeared for the low concentration PVB, while the conductivity of the composite fibers increased and the viscosity decreased. The results indicate that increasing the PVB concentration can reduce beaded fibers. The high conductivity of the solvent is helpful to ion diffusion, and reduces the resistance. However, the high viscosity of the solvent may make it more difficult for the ions to diffuse, and thus reduce conductivity.[17] In Figure 2(b–e), as the concentration of PVB increased, bead-on-string structures could be observed with a reduced density of

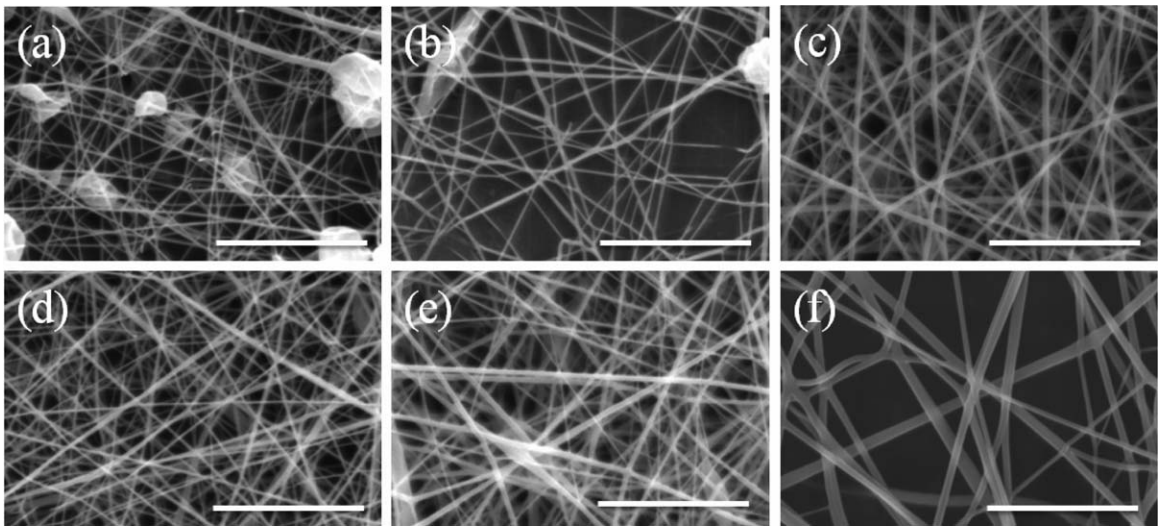

Figure 2. SEM images (scale bar = 5 μm) of PVB/SnS composite fibers with different PVB concentrations: (a) 6, (b) 7, (c) 8, (d) 9, (e) 10%, and (f) pure PVB fiber.

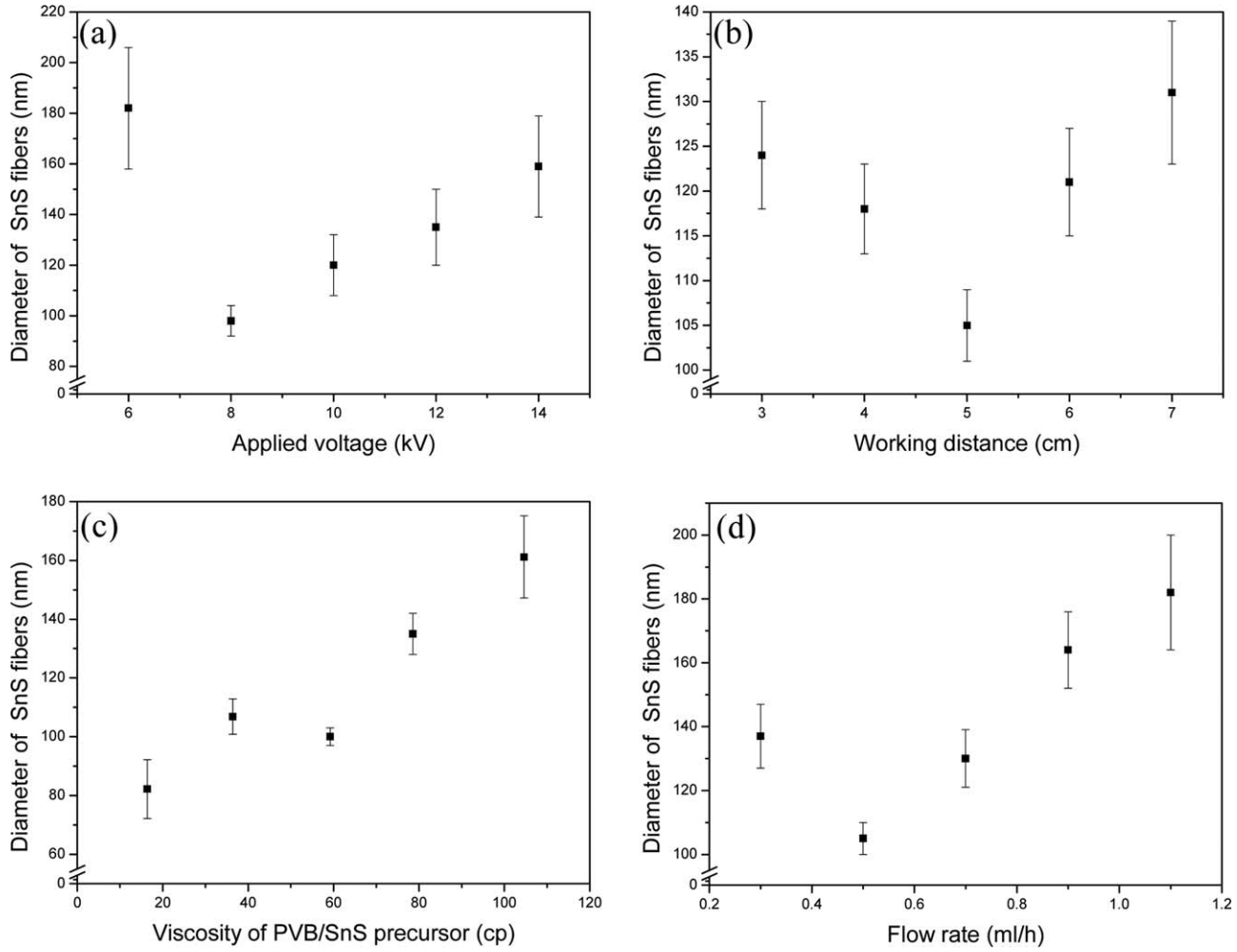

Figure 3. Diameters of PVB/SnS composite fibers for various (a) applied voltages, (b) working distances, (c) viscosities, and (d) flow rates.

beads. In Figure 2(c), for a PVB concentration of 8%, PVB/SnS composite fibers with smooth surfaces were obtained. As the PVB concentration increased, so the quantity of smooth fibers also rose. However, as shown in Figure 2(e), when the concentration of PVB was increased to 10%, the diameter of the fibers increases slightly and their thickness is uneven.[18,19] Figure 2(f) shows an SEM image of pure PVB fibers with relatively smooth surfaces and large diameters. The high conductivity of the solvent is helpful to ion diffusion, and reduces the resistance. The pure PVB precursor solution has no additional ion to increase the conductivity, the pure PVB fibers have large diameters than other PVB/SnS composite fibers.

In Figure 3(a–d) four parameters that might influence the diameter of the electrospun PVB/SnS composite fibers were studied. In Figure 3(a), as the applied voltage was gradually increased from 6 to 14 kV, the diameters of the PVB/SnS composite fibers also rose. It is likely that the diameters of the fibers obtained a narrow distribution due to the balance among the Coulombic, viscoelastic, and surface tension forces. Further increases in the applied voltage would augment the Coulombic force in the electrospun PVB/SnS composite fibers, but reduce the viscoelastic force. This might result in an increased possibility of the breakage of an over-stretched and charged jet during its flight to the target.[19–22] In this work, the most suitable applied voltage for preparing PVB/SnS composite fibers was 8 kV.

In Figure 3(b), the working distance between the needle tip and the collection board was measured, which is correlated with the electric field in the electrospinning process. The results show that as the working distance was increased, the electric field was reduced and the diameter of PVB/SnS composite fibers became finer.[23] Note that if the working distance is significantly reduced or extended (e.g., by 10 cm), no fibers can be formed, and for the latter this is because the force of gravity is greater than the attraction of the electric field. As a consequence, the most suitable working distance for the preparation of PVB/SnS composite fibers was 5 cm.

Figure 3(c) shows that as the viscosity of the electrospun PVB/SnS composite solution was increased, the quantity of beaded fibers was simultaneously reduced, while the diameter of PVB/SnS composite fibers became fine and uniform.[24–27] Note that if

the viscosity is significantly increased, beaded fibers with a rough surface start to be produced.[18,19,28] Under these circumstances, the most suitable viscosity for preparing PVB/SnS composite fibers was about 59.2 cp.

Figure 3(d) shows that as the flow rate of the electrospun PVB/SnS composite solution was increased, the diameter of the PVB/SnS composite fibers also grew.[19,27,29] When the flow rate was higher than 2 mL/h, beaded fibers started to form. As a result, the most suitable flow rate for preparing PVB/SnS composite fibers was 0.5 mL/h.

Thermal Behavior and Structure of PVB/SnS Fibers Produced by Electrospinning

The electrospun PVB/SnS composite solution was then subjected to a sintering process in order to remove PVB and obtain pure SnS fibers. Before the sintering treatment, thermal analysis of the electrospun PVB/SnS composite fibers was performed. Figure 4(a) shows the TGA curves of the PVB/SnS composite fibers and pure PVB fibers. Pure PVB fibers can be evaporated at about 400°C, whereas the weight loss from the PVB/SnS composite fibers started from about 200°C and reached 74.5% at about 700°C. The weight loss from room temperature to 200°C can be attributed to the condensation reaction of SnS precursor to remove OH and the weight loss from 200 to 400°C due to the impurities removal, while that between 400 and 500°C can be attributed to the loss of the oxidation of sulfides[30] and thermal decomposition of the PVB chains. At the later stage from 500 to 700°C, the evaporation of excess S occurs.[31] Above 700°C (up to 800°C in this study), it is most likely that the crystalline structure of the SnS fibers is altered.

Figure 4(b) shows the XRD diffraction patterns of the PVB/SnS composite fibers sintered at 300, 400, and 500°C for 1 h in N_2 atmosphere. The results indicate that the SnS structure remained after the sintering treatment, whereas XRD diffraction pattern (based on JCPDS 39–0354) became clearer and the crystallite sizes increased as the sintering temperature reached 500°C. Note that the diffraction pattern for polycrystalline SnS fibers corresponds to the crystallographic planes of (110), (120), (021), (101), (111), (131), (141), (002), (211), (112), (122), (042), (251), and (080). The average crystal domain size of the as-synthesized SnS fibers, calculated by Scherrer's equation ($D = K\lambda/(B.\cos\theta)$; $K = 0.89$, $\lambda = 0.15418$ nm, $B =$ FWHM, $\theta =$ diffraction angle) and based on the (111) peak, was about 16 nm.

Figure 4(c) shows the SEM image of PVB/SnS composite fibers with the addition of 8% PVB, followed by sintering at 500°C for 1 h in N_2 atmosphere. The as-synthesized SnS fibers are smooth, but fragile. It is very likely that due to the removal of PVB from the SnS matrix, pure SnS fibers became mesoporous and significantly reduced the continuity or unity of the bulk fibers. Note that a mesoporous material contains pores with diameters between 2 and 50 nm.[32]

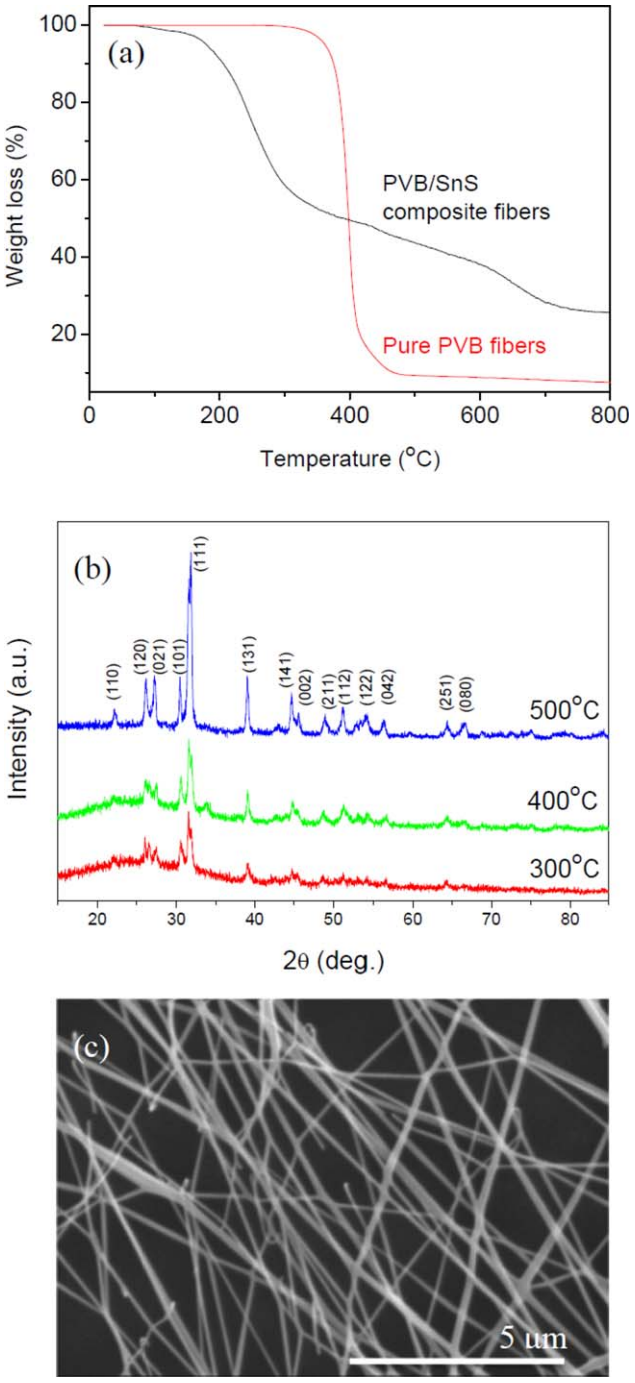

Figure 4. (a) Thermogravimetric analysis (TGA) curves of PVB/SnS composite fibers and pure PVB fibers, (b) XRD pattern of PVB/SnS composite fibers after sintering at 300, 400, and 500°C for 1 h, and (c) SEM image of PVB/SnS composite fibers, e.g., after sintering at 500°C for 1 h. [Color figure can be viewed in the online issue, which is available at wileyonlinelibrary.com.]

Characterization of SnS Mesoporous Fibers

Figure 5 shows TEM micrographs of the as-prepared SnS mesoporous fibers (i.e., electrospun at 8 kV). Figure 5(a,b) show that the SnS mesoporous fibers after calcination at 500°C for 1 h were composed of multilayered particles, with signs of polyhedrons being closely packed and located within the fibers. Figure 5(c) shows an HR-TEM image of a SnS mesoporous fiber, in which it can be seen that the spacing of the crystal lattice was about 0.28 nm, which is mostly consistent with the

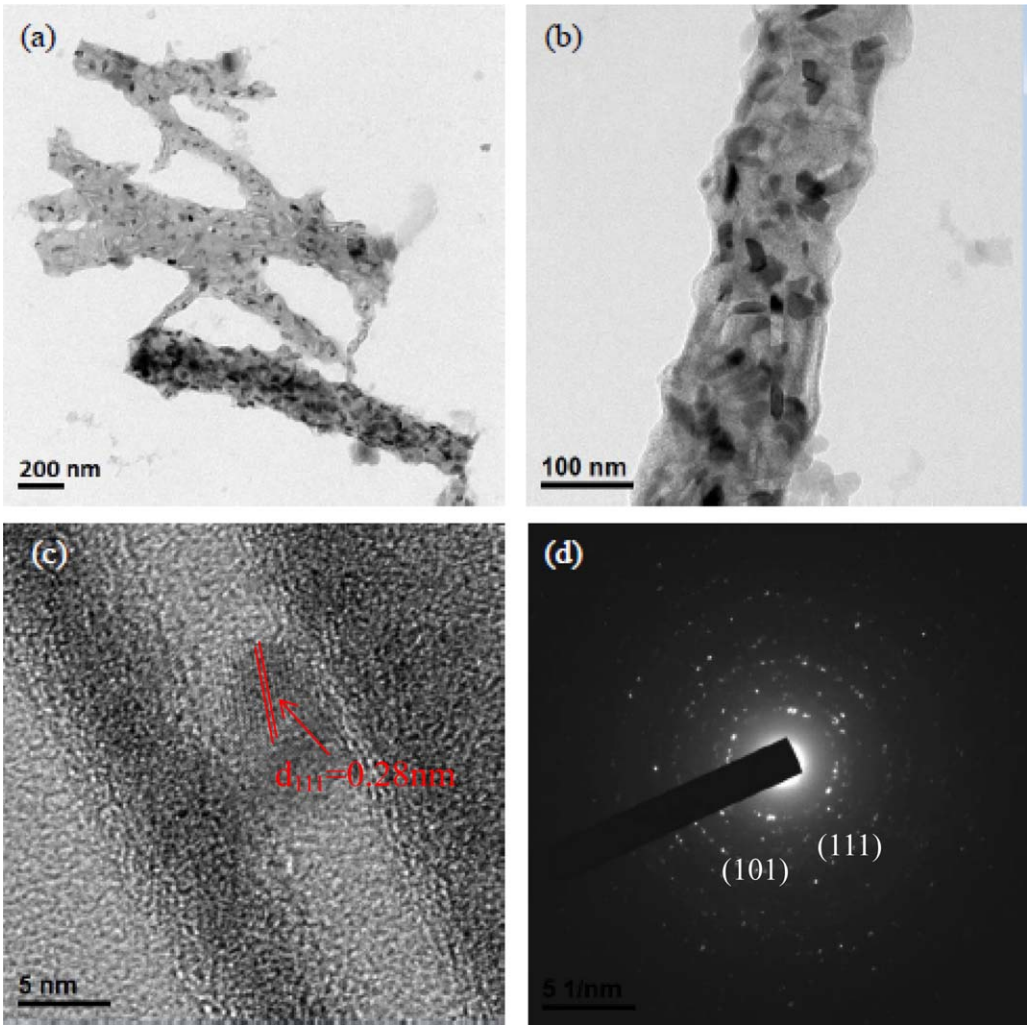

Figure 5. (a) and (b) TEM, (c) HR-TEM, and (d) SAED micrographs of SnS mesoporous fibers after calcination at 500°C for 1 h. [Color figure can be viewed in the online issue, which is available at wileyonlinelibrary.com.]

crystal lattice plane of SnS (111). In Figure 5(d), the SAED image of a SnS mesoporous fiber confirms the presence of the (101) and (111) planes, and indicates that it is a multi-crystalline structure. As determined by EDS, the average composition ratio of the SnS mesoporous fibers, prepared by an electrospinning route, is estimated to be Sn : S = 1.16 : 1, which is close to the perfect element ratio for the stoichiometric SnS structure.

Figure 6 shows the UV–vis spectrum for the as-synthesized orthorhombic SnS mesoporous fibers. The absorbance onset was determined by plotting $(ahv)^2$ versus hv (a: absorbance, h: Planck's constant, and v: frequency). The optical absorbance spectra were then obtained for SnS mesoporous fibers dispersed in ethanol with the energy gap of about 1.49 eV. The as-prepared SnS mesoporous fibers with an appropriate energy gap are thus a supporting matrix with a very high surface area that can increase the amount of internal reflections, and hence increase the probability of light absorption, making it suitable for use in a thin film solar cell. In addition, the absorption energy is placed in the visible light region, which also shows

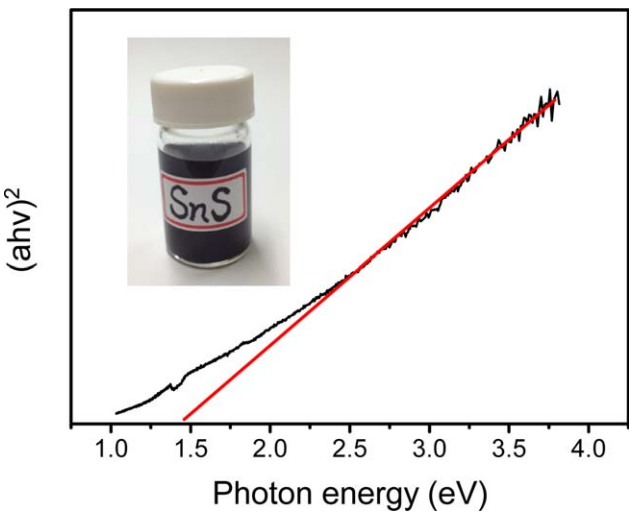

Figure 6. Dependence of $(ahv)^2$ on photon energy (eV) in the case of as-synthesized SnS mesoporous fibers. [Color figure can be viewed in the online issue, which is available at wileyonlinelibrary.com.]

good potential for use in thin film solar cells, with high efficiency under visible light absorption.

CONCLUSION

The optimized parameters to synthesize PVB/SnS composite fibers were set as an applied voltage of 8 kV and a working distance of 5 cm, with the viscosity of 59.2 cp (8 wt % PVB) and flow rate of 0.5 ml/h. The SnS mesoporous fibers without PVB were thereafter fabricated via an electrospinning route, followed by sintering at 500°C for 1 h. The as-prepared SnS mesoporous fibers exhibited an orthorhombic structure with good crystallinity. Their optical absorption showed the presence of direct transition with a band gap energy of 1.49 eV, which means that it is suitable for use as a solar energy light absorption material. The SnS mesoporous fibers with an appropriate energy gap also provide a supporting matrix with a very high surface area to increase internal reflections. In addition, their absorption energy is in the visible light region, which also shows good potential for use in thin film solar cells, with high efficiency under visible light absorption.

ACKNOWLEDGMENTS

Authors thank the Ministry of Science and Technology of Taiwan for financial support, under grant no. MOST 103-2113-M-024-001 and 101-2321-B-006-01.

REFERENCES

1. Katagiri, H.; Jimbo, K.; Maw, W. S.; Oishi, K.; Yamazaki, M.; Araki, H.; Takeuchi, A. *Thin Solid Films* **2009**, *517*, 2455.
2. Ramakrishna Reddy, K. T.; Koteswara Reddy, N.; Miles, R. W. *Sol. Energy Mater. Sol. Cells.* **2006**, *90*, 3041.
3. Sharon, M.; Basavaswaran, K. *Solar Cells.* **1987**, *20*, 323.
4. Thangaraju, B.; Kaliannan, P. *J. Phys. D: Appl. Phys.* **2000**, *33*, 1054.
5. Ramakrishna Reddy, K. T.; Purandhara Reddy, P. *Mater. Lett.* **2002**, *56*, 108.
6. Nwofe, P. A.; Ramakrishna Reddy, K. T.; Sreedevi, G.; Tan, J. K.; Forbes, I.; Miles, R. W. *Energy Procedia* **2012**, *15*, 354.
7. Nair, M. T. S.; Nair, P. K. *Semicond. Sci. Technol.* **1991**, *6*, 132.
8. Mariappan, R.; Mahalingam, T.; Ponnuswamy, V. *Optik* **2011**, *122*, 2216.
9. Koktysh, D. S.; McBride, J. R.; Rosenthal, S. J. *Nanoscale Res. Lett.* **2007**, *2*, 144.
10. Li, D.; Wang, Y.; Xia, Y. *Nano Lett.* **2003**, *3*, 1167.
11. Liu, R. L.; Ye, H. Y.; Xiong, X. P.; Liu, H. Q. *Mater. Chem. Phys.* **2010**, *121*, 432.
12. Wang, W.; Lu, X. F.; Li, Z. Y.; Lei, J. Y.; Liu, X. C.; Wang, Z. J.; Zhang, H. N.; Wang, C. *Adv. Mater.* **2011**, *23*, 5109.
13. He, T. S.; Zhou, Z. F.; Xu, W. B.; Cao,Y.; Shi, Z. F.; Pan, W. P. *Compos. Sci. Techno.* **2010**, *70*, 1469.
14. Bhattacharjee, S.; Paria, M. K.; Maiti, H. S. *J. Mater. Sci.* **1993**, *28*, 6490.
15. Mrkvičková, L.; Daňhelka, J.; Pokorný, S. *J. Appl. Polym. Sci.* **1984**, *29*, 803.
16. Ramakrishna Reddy, K. T.; Koteswara Reddy, N.; Miles, R. W. *Sol. Energy Mater. Sol. Cells.* **2006**, *90*, 3041.
17. Ruenraroengsak, P.; Florence, A. T. *Int. J. Pharm.* **2005**, *298*, 361.
18. Reneker, D. H.; Yarin, A. L.; Fong, H. *J. Appl. Phys.* **2000**, *87*, 4531.
19. Li, D.; Xia, Y. *Nano Lett.* **2003**, *3*, 555.
20. Wannatong, L.; Sirivat, A.; Supaphol, P. *Polym. Int.* **2004**, *53*, 1851.
21. Wu, H.; Pan, W. *J. Am. Ceram. Soc.* **2006**, *89*, 699.
22. Baumgartyen, P. K. *J. Colloid Interface Sci.* **1971**, *36*, 71.
23. Lee, K. H.; Kim, H. Y.; La, Y. M.; Lee, D. R.; Sung, N. H. *J. Polym. Sci. Part B: Polym. Phys.* **2002**, *40*, 2259.
24. Fong, H.; Chun, I.; Reneker, D. H. *Polymer* **1999**, *40*, 4585.
25. Liu, H.; Hsieh, Y. L. *J. Polym. Sci. Part B: Polym. Phys.* **2002**, *40*, 2119.
26. Zong, X.; Kim, K.; Fang, D.; Ran, S.; Hsiao, B. S.; Chu, B. *Polymer* **2002**, *43*, 4403.
27. Lee, K. H.; Kim, H. Y.; Bang, H. J.; Jung, Y. H.; Lee, S. G. *Polymer* **2003**, *44*, 4029.
28. Lee, K. H.; Kim, H. Y.; Ryu, Y. J.; Kim, K. W.; Choi, S. W. *J. Polym. Sci. Part B: Polym. Phys.* **2003**, *41*, 1256.
29. Megelski, S.; Stephens, J. S.; Chase, D. B.; Rabolt, J. F. *Macromolecules* **2002**, *35*, 8456.
30. Majeed Khan, M. A.; Kumar, S.; Alhoshan, M.; Al Dwayyan, A. S. *Opt. Laser Technol.* **2013**, *49*, 196.
31. Hsu, K. C.; Liao, J. D.; Yang, J. R.; Fu, Y. S. *CrystEngComm.* **2013**, *15*, 4303.
32. Rouquerol, J.; Avnir, D.; Fairbridge, C. W.; Everett, D. H.; Haynes, J. H.; Pernicone, N.; Ramsay, J. D. F.; Sing, K. S. W.; Unger, K. K. *Pure Appl. Chem.* **1994**, *66*, 1739.